Original paper

Kogarkoite, Na$_3$(SO$_4$)F, from the Shalo hot spring, Main Ethiopian Rift: implications for F-enrichment of thermal groundwater related to alkaline silicic volcanic rocks

Vladimír ŽÁČEK[1*], Vladislav RAPPRICH[1], Jiří ŠÍMA[2], Radek ŠKODA[1, 3], František LAUFEK[1], Firdawok LEGESA[4]

[1] Czech Geological Survey, Klárov 3, 118 21 Prague 1, Czech Republic; vladimir.zacek@geology.cz

[2] Aquatest a.s., Geologická 4, 152 00 Prague 5, Czech Republic

[3] Department of Geological Sciences, Masaryk University in Brno, Kotlářská 2, 611 37 Brno, Czech Republic

[4] Geological Survey of Ethiopia, P.O. Box 2302, Addis Ababa, Ethiopia

*Corresponding author

Kogarkoite, anhydrous monoclinic sodium fluorosulphate, was identified as a white granular coagulate in the Shalo hot spring situated between the towns of Hawasa and Shashemene, in the central part of the Main Ethiopian Rift in southern Ethiopia. The mineral crystallizes together with trona, Na$_3$(HCO$_3$)(CO$_3$)·2H$_2$O, and opal as white stratified sinter covering the surface of rhyolite chips semi-immerged in Na–HCO$_3$ type thermal water with temperatures of up to 96 °C. The determined chemical composition of kogarkoite is close to the ideal formula Na$_3$(SO$_4$)F and the refined unit-cell parameters are $a = 18.089(2)$ Å, $b = 6.965(1)$ Å, $c = 11.457(1)$ Å, $\beta = 107.72(1°)$, $V = 1374.4(4)$ Å^3.

Increased concentrations of fluorine in groundwater were detected in the area of the rift floor of the central and northern parts of the Main Ethiopian Rift including the wider vicinity of the towns of Shashemene and Hawasa; however, this is the first described occurrence of fluorine-bearing mineral related to hot springs in Ethiopia. The presence of "free" fluorine both in cold groundwater (up to 17 mg/l) and in the Shalo hot spring (40 mg/l) is related to the prevalence of highly alkaline silicic volcanic rocks (namely pantelleritic obsidians) extremely poor in calcium and phosphorus. This prevents fixing of fluorine in apatite or in other stable minerals.

1. Introduction

Kogarkoite, Na$_3$(SO$_4$)F, is a rare monoclinic mineral (space group $P2_1/m$, $Z = 12$) of the sulphohalite group, which is found in several places around the World. Its occurrences belong principally to four paragenetic types: magmatic in alkaline rocks, volcanic sublimate, precipitate from the water of several African alkaline lakes and sinter crystallized from hot springs.

The type locality of kogarkoite is the Umbozero mine in Mt. Alluaiy in the Lovozero Massif, Kola Peninsula, Russia. The mineral was originally described as chlorine-free scheirerite by Kogarko (1961) and later classified as an individual mineral species (Pabst and Sharp 1973). At the type locality, kogarkoite occurs as an accessory mineral in nepheline syenite pegmatite together with villiaumite and many other rare minerals. A similar mineral assemblage was described from an analogous occurrence in Mt. Saint-Hilaire, Quebec (Chao et al. 1991). At Point of Rocks Mesa (Pecks Mesa), Springer, Colfax Co., New Mexico kogarkoite occurs as an accessory mineral in phonolite, consisting of alkali feldspars, zeolites and nepheline (DeMark 1984).

The second type of kogarkoite occurrence is in volcanic sublimates, e.g., at Vulcano, Lipari Islands, Italy (*http://www.mindat.org/locentry-865003.html*) and in the weathered natrocarbonatite of the Mt. Oldoinyo Lengai volcano, Arusha Region, Tanzania (Mitchell 2006).

Kogarkoite was also found as a precipitate in Lake Magadi, Kenya and Lake Natron in Tanzania (Daragi et al. 1983; Nielsen 1999).

Finally, kogarkoite can be found as coagulates from the Hortense hot springs, Chalk Creek, Chaffee County, Colorado (Pabst and Sharp 1973) and in the Shalo hot springs in Central Ethiopian rift, which is objective of this paper.

2. Geological setting

The studied area is located within the Main Ethiopian Rift, a segment of the Miocene–Quaternary intra-continental extensional system – East African Rift System, which extends from Mozambique to Afar (Chorowitz 2005; Abebe et al. 2007). The evolution of the Main Ethiopian Rift has been associated with intense bimodal
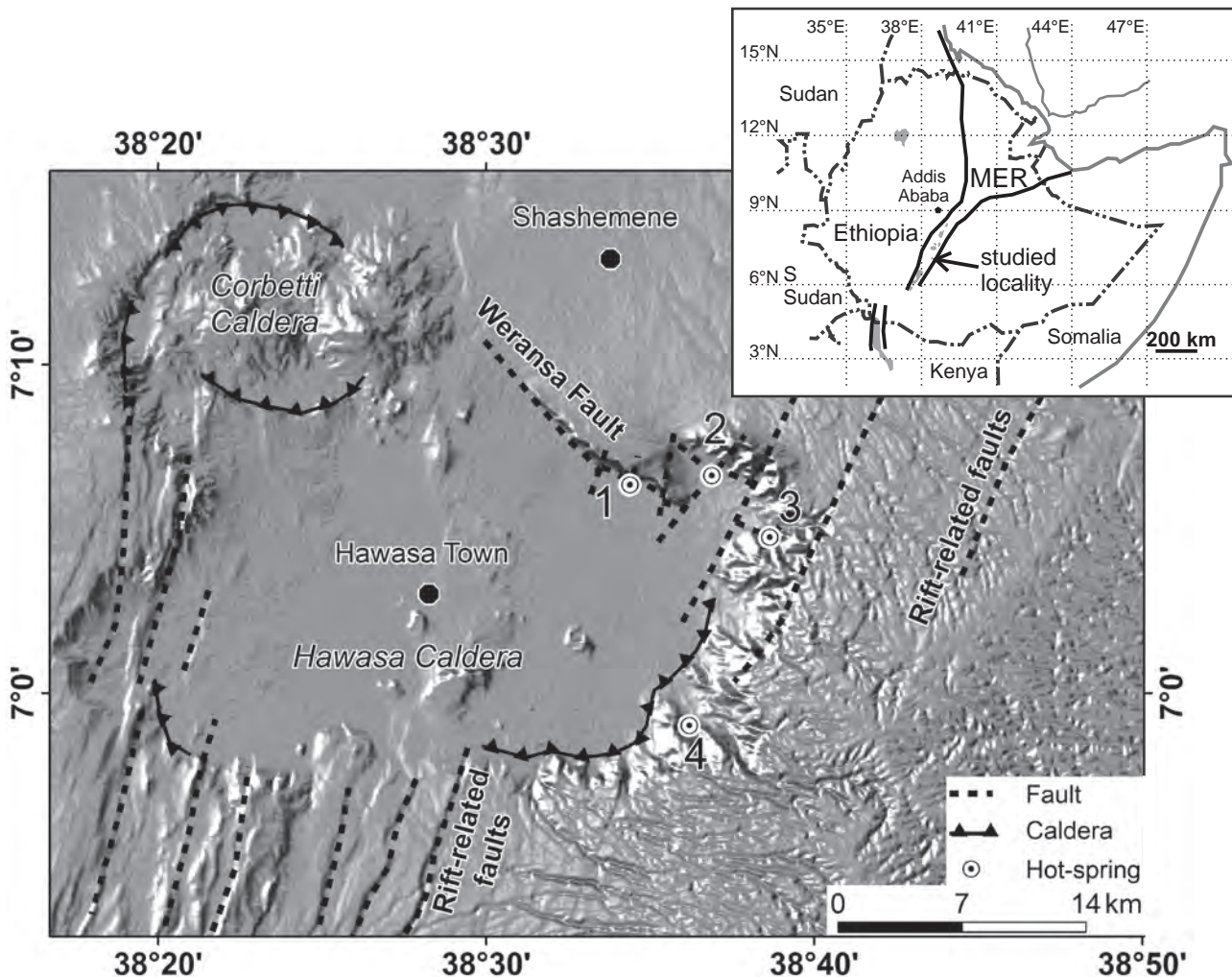
Fig. 1 Location of principal hot-springs on the eastern scarp of the Hawasa Caldera: 1 – Shalo hot springs, 2 – Wesha hot spring, 3 – Wendo Genet hot springs, 4 – Melge Wendo hot spring. The faults and spring locations are taken from Žáček et al. (2014).

volcanic activity, resulting in the formation of linearly aligned mafic volcanic fields (e.g., Rooney et al. 2005; Abebe et al. 2007; Mazzarini et al. 2013) and complex silicic volcanoes. The latter comprise obsidian lava domes and pumiceous deposits, which frequently experienced climactic caldera-forming phases (e.g., Peccerillo et al. 2003; Biggs et al. 2011; Lloyd et al. 2015).

The wider area of the Shalo hot spring is a part of the Hawasa Caldera, located at the eastern edge of the southern part of the Main Ethiopian Rift, in the vicinity of the towns of Shashemene and Hawasa (Fig. 1). The geological evolution of this area prior to the formation of the Hawasa Caldera included both silicic and basic volcanic eruptions. The oldest unit, the Nazret Group of Late Miocene–Pliocene age, is dominated by rhyolitic ignimbrites with subordinate porphyritic trachybasalts in the upper and lower parts of the succession. The ignimbrites of the Nazret Group do not crop out on the surface in the area studied but are exposed in the rift scarps further to the N and E. The ages of the trachybasaltic members of

the Nazret Group, exposed in the area of Wendo Genet, were determined by bulk-rock K–Ar dating at 5.51 ± 3.8 and 10.3 ± 1.4 Ma (Žáček et al. 2014) and a similar age of 9.69 ± 0.7 Ma (bulk-rock) for the older trachybasalts was also presented by Wolde-Gabriel et al. (1990).

The current geology and morphology have mainly resulted from the formation and evolution of the Hawasa Caldera. Several published K–Ar ages (feldspar and bulk-rock) of the ignimbrite eruptions from the Hawasa Caldera vary between 1.1 ± 0.1 and 1.85 ± 0.1 Ma (Wolde-Gabriel et al. 1990, JICA 2012 and Rapprich et al. 2013). The climactic caldera-forming ignimbrite eruptions were followed by extrusions of volcanic domes. The lava domes consisting of microcrystalline rhyolite and obsidian are exposed on the scarps of the Weransa Fault and the Hawasa Caldera in the Wendo Genet area, respectively. The maximum thickness of the Hawasa Caldera eruptive sequence exceeds 600 m, the bulk-rock K–Ar ages vary between 1.02 ± 0.14 and 1.18 ± 0.12 Ma (Žáček et al. 2014).

The formation of the Hawasa Caldera was followed by the younger Corbetti Caldera (Di Paola 1971; Biggs et al. 2011; Rapprich et al. 2013) inset in its north-western corner (Fig. 1). The Corbetti Caldera produced several ignimbrite units during the Middle Pleistocene (0.98 ± 0.26, 0.67 ± 0.13, 0.21 ± 0.01–0.19 ± 0.02 Ma: JICA 2012, Žáček et al. 2014; bulk-rock and bulk-rock with extracted magnetic fraction) reaching up to 700 m of total thickness. The bottom of the Hawasa Caldera infilled with the Corbetti Caldera ignimbrites is intersected by transverse, NW–SE trending Weransa Fault (Fig. 1). Scarce scoria- and tuff-cones with associated basaltic lava flows are scattered over the central, southern and eastern parts of the Hawasa Caldera bottom. Geochronological analysis of these basaltic rocks is somehow problematic, but the geological setting of the basalts overlaying Corbetti ignimbrites suggests the Late Pleistocene age.

The youngest volcanic deposits in the area of interest represent pumices and obsidian lava flows from two post-caldera volcanoes, Chabi and Wendo Koshe (Urji), which emerged within the Corbetti Caldera (DiPaola 1971; Rapprich et al. 2013). The latest pumice eruption occurred ~396 BC (Debebe et al. 2014) and covered the area with a fall deposit with the thickness decreasing eastwards from about 2 m at the Hawasa–Shashemene road to 20 cm in the area of the Shalo hot spring and 10 cm around the Wesha hot spring. A layer of yellowish phreatomagmatic tuff up to 6 m thick and of an uncertain source is embedded between the Pleistocene ignimbrites and the ~396 BC pumice deposit (Žáček et al. 2014). Non-volcanic deposits in the study area mainly represent colluvial sediments and re-sedimented pyroclastic rocks. These polygenetic sediments currently fill the basin of the Hawassa Caldera including the former Chaleleka Lake.

The groundwater infiltration zones in the study area are located on the eastern rift shoulder (eastern plateau) and the thermal waters experienced deep circulation along the rift-marginal and parallel rift faults (Tilahun and Šíma 2013, see Fig. 1). The mineralized thermal springs in the area are associated with travertine in the Wesha (No. 2 in Fig. 1) and Wendo Genet (No. 3 in Fig. 1), silica in the Shalo (No. 1 in Fig. 1) and lower part of Wendo Genet precipitates. The groundwater in the area of the Main Ethiopian Rift becomes highly mineralized with fluorine due to leaching of water-soluble fluorides in loose silicic pyroclastic Pleistocene and Holocene deposits (e.g., Travi and Chernet 1998; Chernet et al. 2001; Ayenew 2008).

3. Methods

3.1. X-ray diffraction (XRD)

The material was separated under a binocular microscope and studied by X-ray powder diffraction. X-ray diffraction data were obtained using a Phillips X'Pert diffractometer (Czech Geological Survey, Prague) in the Bragg-Brentano arrangement using CuK_α radiation (40 kV/40 mA), and a secondary graphite monochromator. The data were collected in the angular range of 2–80° 2θ with a step of 0.02° 2θ for 20 s per step. The material was gently pulverized together with acetone in an agate mortar. To minimize the complicated shape of the background, the sample was placed on a flat silicon wafer from the acetone suspension. The unit-cell parameters were refined from the powder data by whole-profile pattern fitting using the computer program FullProf (Rodríguez-Carvajal 1993). The initial crystallographic data for kogarkoite, trona and halite (which were also present in the sample) were taken from Fanfani et al. (1980), Pertlik (1986) and Nickels et al (1949) respectively.

Fig. 2 View of the eastern (in the foreground) and western branches of the Shalo hot springs from Weransa Ridge with the town of Hawasa on the horizon in 2012. The kogarkoite sample location is marked by an arrow. The image shows how the thermal waters merge in a single brook, which disappears into the marches of the former Chaleleka Lake.

Fig. 3 The eastern branch (eastern "boiling lake") of the Shalo hot springs, close to the kogarkoite occurrence, in 2013. The scarp of the Weransa ridge is formed by rhyolite of the Dino Fm. dated by K–Ar at 1.0–1.2 Ma. This unit is overlain by ignimbrites of the Corbetti Caldera dated at 0.2–0.7 Ma (Žáček et al. 2014).

3.2. Electron microprobe

The carbon-coated polished section of several ~1–2 mm large grains was used for an electron-microprobe study. Chemical microanalyses were performed with a Cameca SX-100 electron microprobe (Joint laboratory of the Masaryk University and the Czech Geological Survey in Brno, Czech Republic) operating in the wavelength dispersion mode with an accelerating voltage of 15 kV, a sample current of 4 nA, and a beam diameter of 5 μm.

The following standards were used: Na – albite, Mg – pyrope, S – $SrSO_4$, Ca – wollastonite, K – sanidine, Fe – almandine, Mn – spessartine, F – CaF_2. The raw data were converted to the concentration using the PaP matrix correction (Pouchou and Pichoir 1985). Silica

was not analysed in the kogarkoite, as the obtained EDS spectra did not indicate significant amounts and traces of Si might have been captured from the surrounding opal.

4. Occurrence

The material containing the later identified kogarkoite was collected from the Shalo hot springs (documentation point SD004: 7.10694°N, 38.56972°E) during geological mapping on a scale of 1 : 50 000 in October 2013 (Žáček et al. 2014). The sampling was undertaken during the dry season. The Shalo hot springs are situated on the rift floor, at the foot of the Weransa Ridge, on the shore of the former Chaleleka Lake, 10 km to the south of Shashemene, southern Ethiopia (Fig. 1). The Shalo hot spring system is located at a crossing of the NW–SE trending Weransa Fault with younger rift-parallel faults (Fig. 1). The hot spring system actually consists of several spring eyes arranged linearly over a distance of some 500 m. There are principally two groups of big springs, forming the eastern and western arms of a small lake producing much vapour, and many smaller dispersed spring eyes with variable discharges. Maximum

Fig. 4 White efflorescence with kogarkoite in a small spring on the western branch of the Shalo spring in 2013.
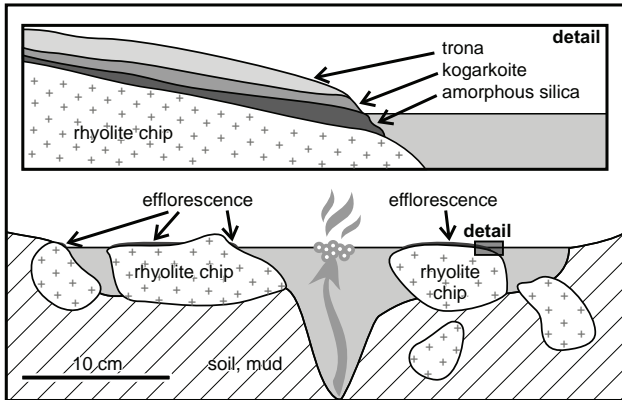
Fig. 5 Schematic section of the hot spring shown in Fig. 4 with the zoned efflorescence containing kogarkoite.

temperature of 96 °C was recorded in the spring UHS-52 (UNDP 1971). The hot water from the springs merges into a single brook, which gradually disappears into the marshes of the former Chaleleka Lake. This observation is in agreement with Di Paola (1971), who stated that the discharge from the group of springs is "not calculable, but high".

The efflorescence occurrence is situated in a small spring on the western branch of the hot lake (Figs 2–3). The white efflorescence is known from several relatively small springs, while on the muddy shore of the neighbouring "lake" it was not observed. Previous studies even reported that efflorescence (sinter deposits) is not present (UNDP 1971).

The minerals occur as a white efflorescence on the chips of rocks semi-immersed in the water. The minerals nucleate at the water level and several mm above the surface of the rock; the completely submerged chips are without efflorescence (Figs 4–5). The surface of the crusts (efflorescence) is white or colourless and can cover several cm^2, with the thickness varying from < 1 mm to ~3 mm.

5. Results

The studied sample represents white efflorescence of up to 3 mm thick grown on a $6 \times 7 \times 4$ cm chip of rhyolite. A stratified structure of efflorescence was observed in the hand specimen and confirmed in the BSE. Microscopic observations showed that the efflorescence consists of three zones (layers) (Fig. 6). The basal layer, nucleated directly on the rock, is 0.1–1.5 mm thick. It is formed by colourless **amorphous silica (opal)** of a glassy massive appearance with a roughly prismatic flake-like decomposition. After a sharp contact, it is followed by a ~1.5 mm thick zone of white fine-grained material, composed of euhedral to subhedral crystals of **kogarkoite** 5–50 μm long (lighter in the BSE) intergrown with subordinate
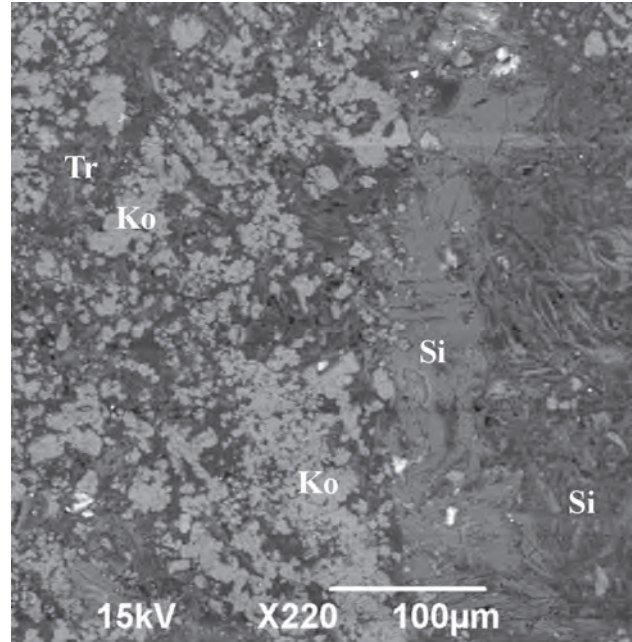

Fig. 6 Back-Scattered Electron (BSE) image of the basal part of the efflorescence composed mainly of amorphous opal (Si) and kogarkoite (Ko) with minor trona (Tr).

trona grains (darker in the BSE, Fig. 6). The surface of the efflorescence is covered by snow-white, extremely delicate skeletal aggregates of **trona** (Fig. 7).

The powder X-ray diffraction study of the white powdery and soft efflorescence (sample SD004a) revealed dominant trona, slightly subordinate kogarkoite and traces of halite. As can be seen in Fig. 8, the strongly
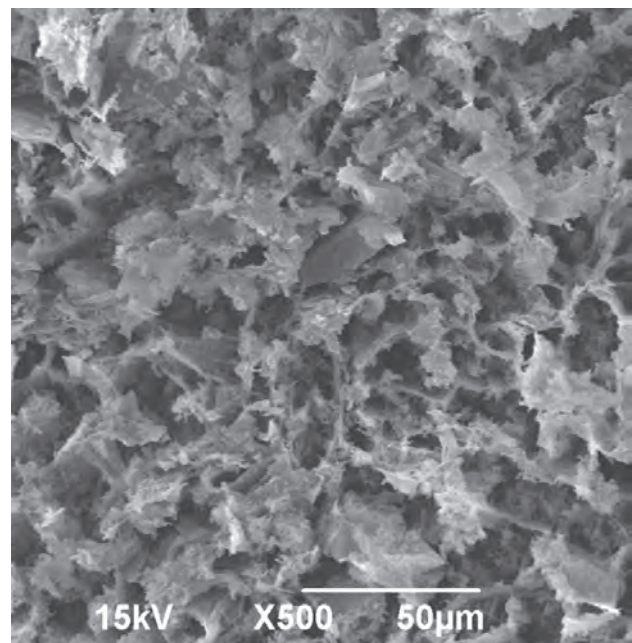

Fig. 7 Back-Scattered Electron (BSE) image of the surface of the efflorescence formed by delicate skeletal aggregates of trona.
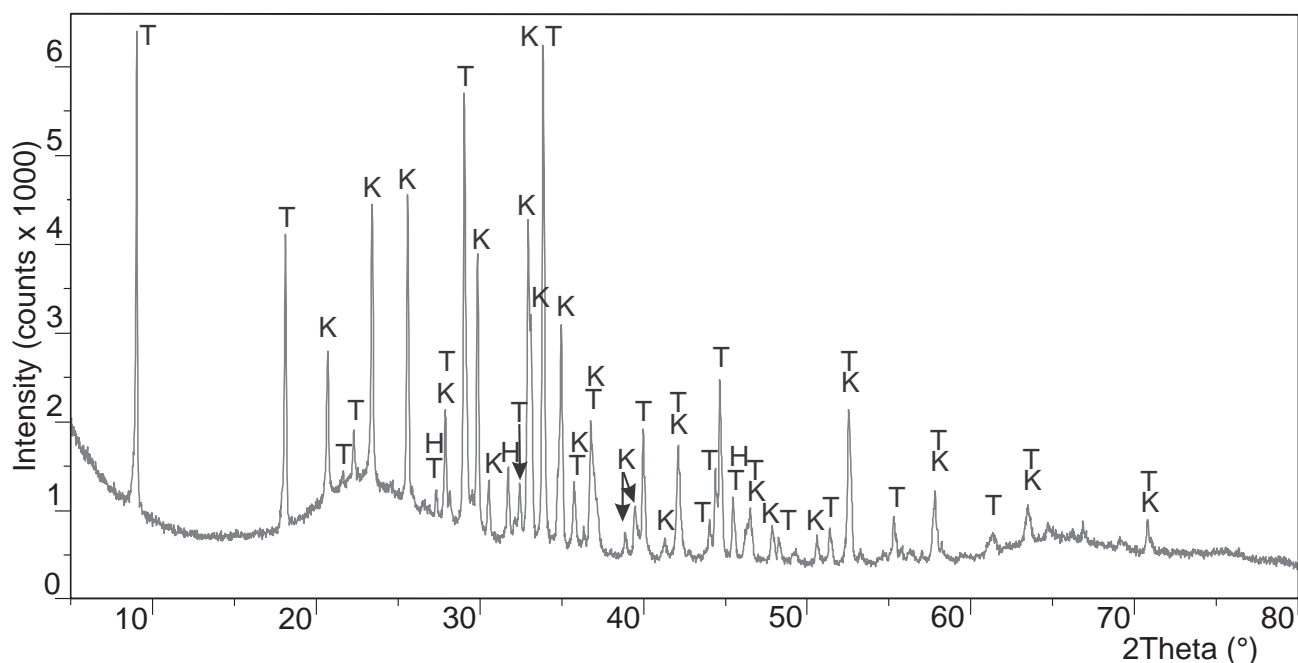
Fig. 8 Powder X-ray diffraction pattern of the sample SD004a containing kogarkoite (K – kogarkoite, T – trona, H – halite).

Tab. 1 Powder X-ray diffraction data for kogarkoite (in Å)

h	k	l		I_{obs}	d_{obs}	I_{calc}	d_{calc}
4	0	0	}	46	4.3004	27	4.3077
0	1	2				59	4.2953
3	1	1	}	87	3.8040	90	3.8058
$\bar{1}$	0	3				41	3.8008
0	0	3				5	3.6376
$\bar{4}$	1	2	}	97	3.4862	100	3.4883
0	2	0				52	3.4824
1	0	3		4	3.3603	5	3.3584
$\bar{5}$	0	3	}	95	2.9949	47	2.9990
3	2	1				96	2.9954
$\bar{6}$	0	2		4	2.9376	9	2.9364
2	2	2		20	2.9295	18	2.9290
3	0	3		100	2.7202	96	2.7213
4	2	0	}	73	2.7061	61	2.7081
$\bar{4}$	0	4				35	2.7075
$\bar{7}$	0	1		29	2.5752	40	2.5754
1	2	3		68	2.5679	88	2.5676
4	0	3		19	2.4386	26	2.4373
5	5	1		14	2.2858	26	2.2866
$\bar{3}$	0	5		9	2.2826	11	2.2843
8	0	0		11	2.1529	18	2.1538
$\bar{7}$	0	5				8	1.9552
$\bar{5}$	3	1	}	14	1.9521	12	1.9539
3	3	3				8	1.9526
6	2	2		10	1.9035	23	1.9029
2	0	6		4	1.9007	6	1.9004
6	3	0		7	1.8057	12	1.8054
1	3	5		2	1.6163	7	1.6166

Diffraction lines of kogarkoite overlapping with trona diffractions and are not shown. Only calculated lines with $I_{calc} \geq 4$ are included. Theoretical data calculated by PowderCell (Kraus and Nolze 2000) from the crystal structure of kogarkoite (Fanfani et al. 1980).

elevated background in the diffraction data between ~15–40° 2Θ, with a weak maximum at ~22° 2Θ, indicates the presence of an amorphous phase (most likely opal).

Sample SD004b from the underlying colourless, glassy and relatively hard material was completely amorphous (opal) with the characteristic elevated background described above. Diffraction data are given in Tab. 1. The refined unit-cell parameters for space group $P2_1/m$ (Tab. 2) are consistent with values reported previously for kogarkoite samples (Pabst and Sharp 1973; Fanfani et al. 1980).

The microprobe analysis yielded a chemistry close to the ideal formula of kogarkoite, $Na_3(SO_4)F$; the slight deviation from the ideal stoichiometry is most probably caused by partial volatilization of the Na during the analysis. The concentrations of CaO range between 0.09 and 0.15 wt. %; FeO, MgO, K_2O are still lower, mostly below 0.10 wt. % (Tab. 3). Chlorine was not detected. The lower analytical totals of some analyses (98.5–99 wt. %) are most probably due to the porosity of the sample and instability of the kogarkoite under electron beam.

Tab. 2 Unit-cell parameters for kogarkoite (space group $P2_1/m$)

	this paper	Pabst and Sharp (1973)	Fanfani et al. (1980)
a [Å]	18.089(2)	18.073	18.074
b [Å]	6.965(1)	6.949	6.958
c [Å]	11.457(1)	11.440	11.443
β [°]	107.72(1)	107.71	107.71
V [Å³]	1374.4(4)	1368.6	1370.9

Tab. 3 Chemical composition of kogarkoite (wt. %) from the Shalo hot spring, southern Ethiopia

No	4	5	7	8
FeO^t	0.03	0.04	0.02	0.02
MnO	0.00	0.00	0.00	0.01
MgO	0.00	0.00	0.11	0.00
CaO	0.13	0.11	0.10	0.12
Na_2O	50.04	49.84	49.14	49.62
K_2O	0.07	0.00	0.00	0.04
SO_3	43.67	43.43	42.92	43.54
F	10.96	10.53	10.79	10.92
–O=F	4.60	4.42	4.53	4.59
Sum	100.29	99.53	98.55	99.68
Fe^{2+}	0.001	0.001	0.000	0.000
Mn	0.000	0.000	0.000	0.000
Mg	0.000	0.000	0.005	0.000
Ca	0.004	0.004	0.003	0.004
Na	2.950	2.965	2.946	2.940
K	0.003	0.000	0.000	0.001
S	0.997	1.000	0.996	0.999
F	1.055	1.022	1.055	1.056
Total	5.009	4.992	5.007	5.000

Formulae based on 5 (O + F) atoms per formula unit

6. Discussion

Kogarkoite occurs together with opal and trona as coagulate in the Shalo hot spring located on the eastern edge of the Hawasa Caldera in the Main Ethiopian Rift. This thermal spring displays the highest temperatures (up to 96 °C), highest concentrations of F^-, SiO_2 and SO_4^{2-}, plus high Na^+ and HCO_3^- and the lowest Ca^{2+} of all of the thermal springs in the vicinity of the towns of Shashemene and Hawasa.

The minerals form a recent sinter on the surface of the rhyolite chips by coagulation, capillary rise and evaporation processes. Poorly soluble amorphous silica (opal, $SiO_2 \cdot nH_2O$) precipitates first, followed by kogarkoite. Finally, water well-soluble trona nucleates on the top of the efflorescence by a combination of capillary rise and evaporation.

The studied kogarkoite has a nearly stoichiometric empiric formula, the elevated CaO (0.09–0.15 wt. %) is notable with respect to the low Ca content in the water and the absence of Ca carbonates in the spring precipitate.

The water chemistry of the Shalo hot spring UHS-52 (T = 96 °C, pH = 3) taken from a study by UNDP (1971) and also given by Žáček et al. (2014) is as follows (mg/l): Na^+ 430, K^+ 44, Ca^{2+} 1, Mg^{2+} 2, HCO_3^- 800, CO_3^{2-} 58, Cl^- 38, F^- 40, SO_4^{2-} 83, SiO_2 137, HBO^- 0.4.

High concentrations of free fluorine in the thermal water are related to the prevailing geochemistry of the surrounding silicic rocks, namely Holocene pyroclastic fall deposits. According to Cronin et al. (2003), the rapidly soluble fluorides in silicic volcanic environs are mainly represented by NaF and $CaSiF_6$ which form tiny coatings on pyroclastic particles (Óskarsson 1980). The high reaction surface of fine-grained or densely vesicular pyroclastic deposits is prone to very rapid leaching.

The following compositional ranges include 9 chemical analyses of silicic rocks from the vicinity of Shashemene (Žáček et al. 2014). All of these rocks contain high concentrations of SiO_2 (69.67–75.16 wt. %), K_2O (4.19–4.76 wt. %), Na_2O (3.52–4.96 %) and F (0.05–0.25 wt. %) as well as extremely low concentrations of CaO (0.12–0.58 wt. %) and P_2O_5 (0.013–0.041 wt. %).

It is a well-known fact that the concentrations of fluorine (fluoride) in the groundwater around Shashemene and Hawasa are generally high. The fluorine concentration in the cold groundwater, including drilled wells, can reach 17 mg/l and tends to decrease with depth (Tadesse and Zenaw 2003; Žáček et al. 2014). This is likely to be an effect of progressive depletion of older volcanic (pyroclastic) rocks in fluorine due their higher age and the longer leaching of fluoride in the past. The thermal waters tend to have high fluorine concentrations (up to 40 mg/l) as elevated temperatures allow intense leaching of acidic rocks and higher dissolution of fluorine (fluoride). There is a direct correlation between the chemical composition of silicic volcanic rocks and high concentrations of fluorine in groundwater. Porous silicic pyroclastic rocks, such as pumice, where fluorine is present as water-soluble sodium fluoride, are considered to represent the main source of leachable fluoride. The rhyolitic rocks are extremely poor in calcium and phosphorus, which prevents fixing of fluorine in apatite or non-leachable calcium fluoride. Rango et al. (2009) stated that fluorine concentrations in groundwater are inversely related to the concentration of calcium, which permits the high mobility of fluorine at low Ca levels in groundwater. This is the case of the Shalo hot spring, which contains 40 mg/l of F but only 1 mg/l of Ca. The elevated concentrations of SO_4 together with high Na content lead to the crystallization of sodium fluorosulphate (kogarkoite) instead of sodium fluoride (villiaumite) following the chemical reaction: $Na_2SO_4 + NaF = Na_3SO_4F$.

A similar occurrence of kogarkoite was found in the Hortense hot springs (up to 83 °C) in Chafee County, Colorado (Pabst and Sharp 1973). The local geology is dominated by strongly zeolitized quartz monzonite. Kogarkoite there crystallizes as a sublimate around steam vents of the hot springs associated with opal, halite and calcite, fluorite, burkeite and trona. The analysis of thermal water yielded a total mineralization of 339 mg/l and elevated concentrations of SiO_2, Na^+, SO_4^{2-}, F^-, and HCO_3^- (Pabst and Sharp 1973), which is very similar to the composition of the thermal water from the Shalo hot springs.

References

Abebe B, Acocella V, Korme T, Ayalew D (2007) Quaternary faulting and volcanism in the Main Ethiopian Rift. J Afr Earth Sci 48: 115–124

Ayenew T (2008) The distribution and hydrogeological controls of fluoride in the groundwater of central Ethiopian rift and adjacent highlands. Environ Geol 54: 1313–1324

Biggs J, Bastow ID, Keir D, Lewi E (2011) Pulses of deformation reveal frequently recurring shallow magmatic activity beneath the Main Ethiopian Rift. Geochem Geophys Geosyst 12: doi: 10.1029/2011GC003662

Chao GY, Grice JD, Gault RA (1991) Silinaite – a new sodium lithium silicate hydrate mineral from Mont Saint-Hilaire, Quebec. Canad Mineral 29: 359–362

Chernet T, Travi Y, Valles V (2001) Mechanism of degradation of the quality of natural water in the lakes region of the Ethiopian rift valley. Water Res 35: 2819–2832

Chorowitz J (2005) The East African rift system. J Afr Earth Sci 43, 379–410

Cronin SJ, Neall VE, Lecointre JA, Hedley MJ, Loganathan P (2003) Environmental hazards of fluoride in volcanic ash: a case study from Ruapehu volcano, New Zealand. J Volcanol Geotherm Res 121: 271–291

Daragi F, Gueddari M, Fritz B (1983) Presence of kogarkoite (Na₃SO₄F) in the salt paragenesis of lake Natron in Tanzania. C R Acad Sci Paris, Serie II, 297: 141–144

Debebe N, Yekoye B, Rapprich V (eds) (2014) Geological hazards and Engineering geology maps of Hosaina NB 37-2. Explanatory notes. Czech Geological Survey, Prague, Aquatest a.s., Prague, Geological Survey of Ethiopia, Addis Ababa, pp 1–148

DeMark RS (1984) Minerals of Point of Rocks, New Mexico. Mineral Rec 15: 150–156

Di Paola GM (1971) Geology of the Corbetti Caldera area (Main Ethiopian Rift Valley). Bull Volcan 35: 497–506

Fanfani L, Giuseppetti G, Tadini C, Zanazzi PF (1980) The crystal structure of kogarkoite, Na₃SO₄F. Mineral Mag 43: 753–759

JICA (Japan International Cooperation Agency) (2012) The Study on Groundwater Resources Assessment in the Rift Valley Lakes Basin in the Federal Democratic Republic of Ethiopia. Unpublished Final Report, Japan International Cooperation Agency (JICA), Kokusai Kogyo Co., Ltd., Ministry of Water and Energy (MoWE), The Federal Democratic Republic of Ethiopia, pp 1–721

Kogarko LN (1961) Chlorine-free schairerite from the nepheline syenites of the Lovozero Massif (Kola Peninsula). Dokl Akad Nauk SSSR 139: 839–841

Kraus W, Nolze G (2000) PowderCell for Windows-Version 2.4 – Structure Visualisation/Manipulation, Powder Pattern Calculation and Profile Fitting. Federal Institute for Materials Research and Testing, Berlin

Lloyd R, Biggs J, Wilks M, Eysteinsson H (2015) An investigation into the temporal and spatial evolution of deformation at Corbetti volcano, Main Ethiopian Rift. Annual Volcanic and Magmatic Studies Group Conference, 5–7th January 2015, Norwich, pp 69

Mazzarini F, Keir D, Isola I (2013) Spatial relationship between earthquakes and volcanic vents in the central-northern Main Ethiopian Rift. J Volcanol Geotherm Res 262: 123–133

Mitchell RH (2006) Mineralogy of stalactites formed by subaerial weathering of natrocarbonatite hornitos at Oldoinyo Lengai, Tanzania. Mineral Mag 70: 437–444

Nickels JE, Fineman MA, Wallace WE (1949) X-ray diffraction studies of sodium chloride–sodium bromide solid solutions. J Phys Chem 53: 625–628

Nielsen JM (1999) East African magadi (trona): fluoride concentration and mineralogical composition. J Afr Earth Sci 29: 423–428

Óskarsson N (1980) The interaction between volcanic gases and tephra, fluorine adhering to tephra of the 1970 Hekla eruption. J Volcanol Geotherm Res 8: 251–266

Pabst A, Sharp WN (1973) Kogarkoite, a new natural phase in the system Na₂SO₄−NaF−NaCl. Amer Miner 58: 116–127

Peccerillo A, Barberio MR, Yirgu G, Ayalew D, Barbieri M, Wu TW (2003) Relationships between mafic and peralkaline silicic magmatism in continental rift settings: a petrological, geochemical and isotopic study of the Gedemsa Volcano, Central Ethiopian Rift. J Petrol 44: 2003–2032

Pertlik F (1986) Ein Vergleich von Ergebnissen routinemaessiger Strukturbestimmungen mittels Roentgen-bzw. Neutronen-Einkristalldaten am Beispiel der Trona, Na₃H(CO₃)₂(H₂O)₂. Mitt Österr mineral Gesell 131: 7–14

Pouchou JL, Pichoir F (1985) "PAP" correction procedure for improved quantitative microanalysis. In: Armstrong

JT (ed) Microbeam Analysis. San Francisco Press, CA, pp 104–106

RANGO T, BIANCHINI G, BECCALUVA L, AYENEW T, COLOMBANI N (2009) Hydro-geochemical study in the Main Ethiopian Rift: new insights to the source and enrichment mechanism of fluoride. Environ Geol 58: 109–118

RAPPRICH V, ČÍŽEK, D, DANIEL K, FIRDAWOK L, HABTAMU B, HROCH T, KOPAČKOVÁ V, MÁLEK J, MALÍK J, MIŠUREC J, ORGOŇ A, ŠEBESTA J, ŠÍMA J, TSIGEHANA T, VERNER K, YEWUBINESH B (2013) Explanation Booklet to the Set of Geoscience Maps of Ethiopia at Scale 1 : 50,000, Sub-sheet 0738-C4 Hawasa. Czech Geological Survey, Prague, Aquatest a.s., Prague, Geological Survey of Ethiopia, Addis Ababa, pp 1–46

RODRÍGUEZ-CARVAJAL J (1993) Recent advances in magnetic structure determination by neutron powder diffraction. Physica B 192: 55–59

ROONEY TO, FURMAN T, YIRGU G, AYALEW D (2005) Structure of the Ethiopian lithosphere: xenolith evidence in the Main Ethiopian Rift. Geochim Cosmochim Acta 69: 3889–3910

TADESSE D, ZENAW T (2003) Hydrology and Engineering Geology of Awasa Lake Catchment. Geological Survey of Ethiopia, Addis Ababa, pp 1–67

TILAHUN K, ŠÍMA J (2013) Hydrogeological and Hydrochemical Maps of Hosaina NB 37-2. Explanatory Notes. Aquatest a.s., Prague, pp 1–194

TRAVI Y, CHERNET T (1998) Fluoride Contamination in the Lakes Region of the Ethiopian Rift: Origin, Mechanism and Evolution. IAEA (International Atomic Energy Agency) Report, Vienna, TECDOC-1046: 95–105. Accessed on 13 August, 2015, at *http://www.iaea. org/inis/collection/NCLCollectionStore/_Public/ 29/062/29062773.pdf*

WOLDE-GABRIEL G, ARONSON JL, WALTER RC (1990) Geology, geochronology, and rift basin development in the central sector of the Main Ethiopian Rift. Geol Soc Am Bull 102: 439–458

ŽÁČEK V, RAPPRICH V, AMAN Y, BERHANU B, ČÍŽEK D, DEREJE K, ERBAN V, EZRA T, FIRDAWOK L, HABTAMU M, HROCH T, KOPAČKOVÁ V, KYCL P, MIŠUREC J, ORGOŇ A, PÉCSKAY Z, ŠÍMA J, TAREKEGU D, VERNER K (2014) Explanation Booklet of the Set of Geoscience Maps of Ethiopia at scale 1 : 50 00, Sub-sheet 0738-D3 Shashemene: Geological Map, Hydrogeological Map, Geohazards Map. Czech Geological Survey, Prague, Aquatest a.s., Prague, Geological Survey of Ethiopia, Addis Ababa, pp 1–52